Rare Metal Materials and Engineering
Volume 48, Issue 3, March 2019
Available online at www.rmme.ac.cn

Science Press

Cite this article as: Rare Metal Materials and Engineering, 2019, 48(3): 0711-0715.

ARTICLE

Numerical Simulation of Electron Beam Melting Vanadium Alloys by Finite Element Method

Su Bin, Chen Daoming, Wang Zhenhong, Ma Rong, Li Yufei, Xia Shengquan

China Academy of Engineering Physics, Jiangyou 621907, China

Abstract: A mathematical model was developed to investigate the electron beam melting (EBM) process of vanadium alloys. The temperature distribution of molten V-4Cr-4Ti alloy was obtained using the model. The effects of different parameters of electron beam melting process on the temperature field and the shape of molten pool were studied. The results show that the temperature field and the shape of the molten pool are influenced by the melting power and scanning radius. With increasing the melting power, the maximum melt temperature increases linearly and the width and depth of molten pool gradually increase. With increasing the scanning radius, the maximum melt temperature increases first and then decreases. The optimized parameters of refining vanadium were obtained, and the accuracy of the model was validated by the experimental data.

Key words: electron beam melting; vanadium alloys; temperature field; numerical simulation

Vanadium alloys have been investigated as potential constructive materials for the first wall blanket of the fusion reactors because of their low induced activation characteristics, high temperature strength and high thermal stress factors [1,2]. Vanadium alloys are commonly processed by a vacuum consumable arc-melting (VAR) method[3-5]. However, the contents of the impurity elements such as oxygen, nitrogen and carbon in vanadium alloys are hard to control by VAR. The electron beam melting (EBM) is a widely used method of special electric metallurgy, and an effective way for removing the volatile impurities from vanadium alloys.

In comparison with other metallurgic methods, the EBM provides a better refining effect for the casting metal from solvable gases and non-metal inclusions, as well as metal components that are easily evaporated [6,7]. The results of EBM of the metals and alloys are in close connection with the temperature distribution of the treated ingot, the melting pool shape and the volume and convection of the liquid metal [8]. With the advancements of computer technology, numerical modeling and simulation have been widely used as powerful tools to better understand the melting process [9]. Some numerical simulation researches [6,8,10-13] have been done to investigate the temperature distribution during EBM.

In this paper, numerical simulations of temperature field during electron beam melting of vanadium alloys were carried by ANSYS software. The effects of the melting power and scanning radius on the temperature and the shape of the molten pool were investigated. The optimized parameters of refining vanadium were obtained, and the accuracy of the model was validated by the experimental data.

1 Model Description

Fig.1 schematically illustrates the electron beam melting process. In the EBM process of vanadium alloys, the raw material is produced by a vacuum self-consuming arc melting furnace. The process is held in vacuum chamber with one

Received date: March 15, 2018
Foundation item: Science and Technology Development Foundation of Chinese Academy of Engineering Physics (2015B0203031); Science Challenge Program (TZ20160040201)
Corresponding author: Xia Shengquan, Ph. D., Institute of Materials, China Academy of Engineering Physics, Jiangyou 621907, P. R. China, Tel: 0086-816-3626940, E-mail: xiashengquan2001@163.com

or several electron-optical systems, in which intense electron beams are generated and directed onto the raw material bar and the molten pool on the top surface of cast ingot. The raw material in form of bars is fed horizontally in vacuum environment and is melted directly to the withdrawal bottom of a copper water cooled crucible. The surface of the molten metal in the crucible is also heated by the electrons. The electron beam and the high vacuum provide degassing and high level of refining, as well as homogeneity of the chemical composition and optimal structure of the cast ingots[6].

A finite element based heat transfer model was developed to describe the heat transfer occurring in the ingot, bottom block and copper crucible. It has been assumed that the heat flow in the process is steady-state symmetric in the circumferential direction. The heat flow in the ingot, starter block and copper support in the radial direction r and axial direction z can be described as follows[10]:

$$\frac{1}{r}\frac{\partial}{\partial r}\left(kr\frac{\partial T}{\partial r}\right)+\frac{\partial}{\partial z}\left(k\frac{\partial T}{\partial z}\right)+\dot{Q}=\rho C_{\mathrm{p}}\frac{\partial T}{\partial t} \quad (1)$$

where T is the temperature, k is the thermal conductivity, ρ is the density, C_{p} is the specific heat, and $\dot{Q}$ is the volumetric latent heat that is associated with the solidification phase transformation.

The input heat flux, q_{EB} (W/m^2), from the electron beam gun was described using a Gauss function[10]:

$$q_{\mathrm{EB}}=\mu_{\mathrm{EB}}\eta_{\mathrm{power}}C\mathrm{e}^{\left[\frac{-(r-R)^2}{2\sigma^2}\right]} \quad (2)$$

where μ_{EB} is the EB power transfer efficiency, η_{power} is the normalized EB power, C is a pre-exponential constant, r is the location radius, R is the scanning radius, and σ is the standard deviation of the distribution. The constant C is chosen to ensure the correct total beam power for a given value of σ.

A set of appropriate boundary conditions for the four regions of the boundary ingot surfaces are chosen to account for the radiation losses and heating beam energy distribution with a correction of the electron energy losses. The geometry configuration of the mathematical model with boundary conditions is shown schematically in Fig.2. The geometry dimensions of the mathematical model refer to the actual dimensions of the experiment.

2 Results and Discussion

In this work, numerical simulations of electron beam melting process of V-4Cr-4Ti alloy were carried out by ANSYS software. The 2D axisymmetric mesh used in the analysis, shown in Fig.3, contains 2518 nodes and 2712 elements. The ingot diameter is 50 mm and ingot length is 200 mm. The material properties of V-4Cr-4Ti alloy and copper crucible used in the model are summarized in Table 1.

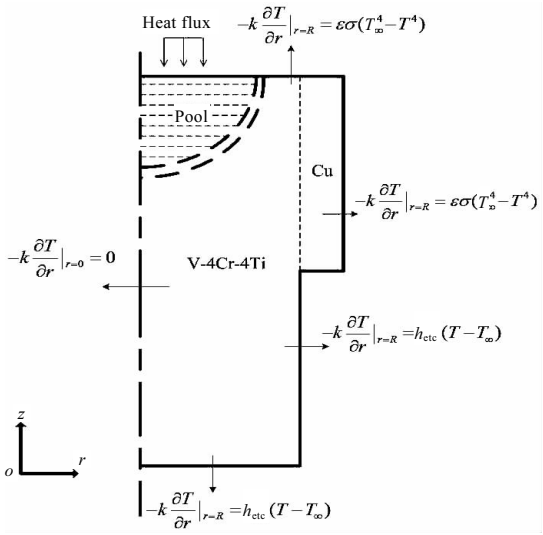

Fig. 2 Geometry configuration of the model with boundary conditions

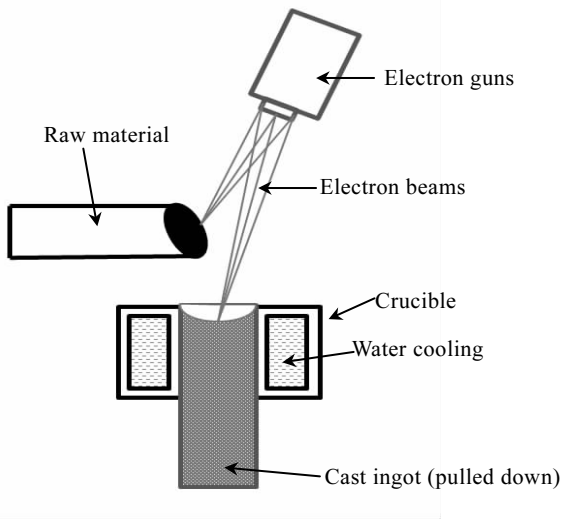

Fig. 1 Schematic illustration of electron beam melting process

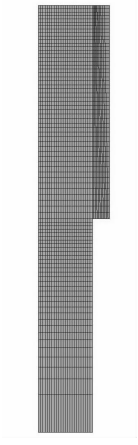

Fig.3 Finite element mesh model used in the analysis

Table 1 Main physical parameters of V-4Cr-4Ti alloy and copper crucible[4,10,13]

Definition and symbols	Materials	Values
Density, ρ/kg·m^{-1}	V-4Cr-4Ti	6100
	Cu	8960
Specific heat, C_p/J·(kg·K)$^{-1}$	V-4Cr-4Ti	535
	Cu	390
Thermal conductivity, k/	V-4Cr-4Ti	34.5
W·(m·K)$^{-1}$	Cu	401
Liquidus temperature, T_L/K	V-4Cr-4Ti	1940

Fig.4 shows temperature distributions in a cross-section of the cast ingot during electron beam melting at different scanning radii and melting power of 60 kW. Fig.5 shows heat flux distribution at different scanning radii. It can be seen that the distance from the center of heat flux distribution to the center of ingot increases with increasing the scanning radius, and the distance from the molten pool to the center of ingot also increases. The results also show that there might be a non-melting zone on the surface of ingot, when scanning radius enlarges to a certain value. Fig.6 shows the relation of melting power and scanning radius with maximum melt temperature. It can be seen that as the scanning radius increases, the max melt temperature increases first and then decreases.

Fig.7 shows temperature distributions in a cross-section of the cast ingot during electron beam melting with different melting powers. Fig.8 shows the maximum melt temperature and minimum melt temperature at different melting powers. It can be seen that the max melt temperature increases linearly with increasing the melting power, and the variation of the minimum melt temperature is not obvious. With increasing the melting power, the width and depth of molten pool gradually increase.

As is known, the volatile impurities can be easily removed with a high melt temperature and a large area of the molten pool. However, with increasing the melting temperature, the loss rate of the base metal also increases and the life of copper crucible decreases. The removal of the volatile impurities increases with the increment of the width and depth of molten pool. However, refining effectiveness will be affected when the depth of molten pool reaches a certain value.

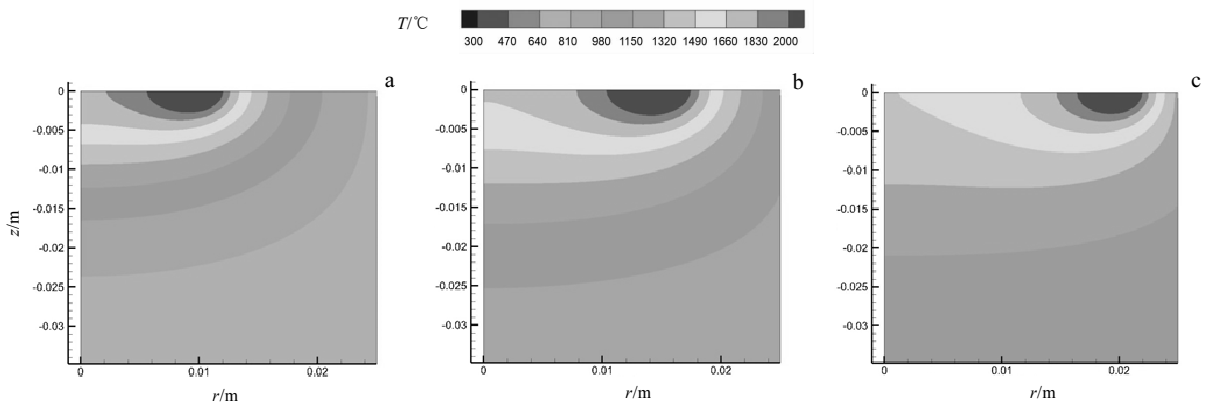

Fig.4 Temperature distribution at the beam power of 60 kW and different scanning radii: (a) r=10 mm, (b) r=15 mm and (c) r=20 mm

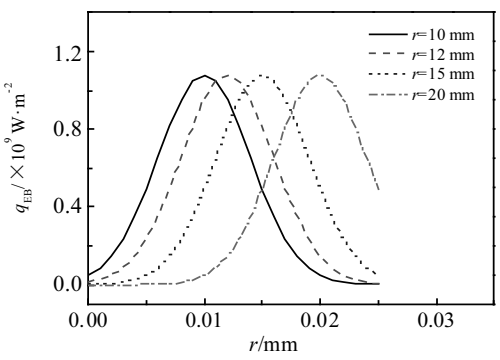

Fig.5 Heat flux distribution at the beam power of 60 kW

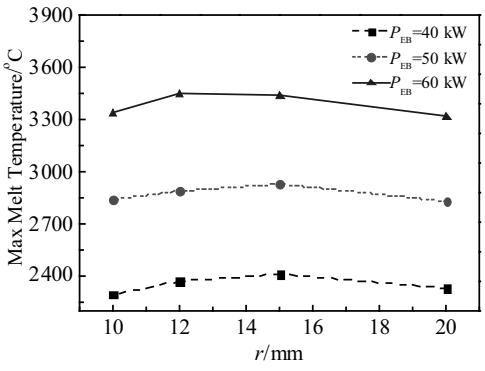

Fig.6 Relation of melting power and scanning radius with maximum melt temperature

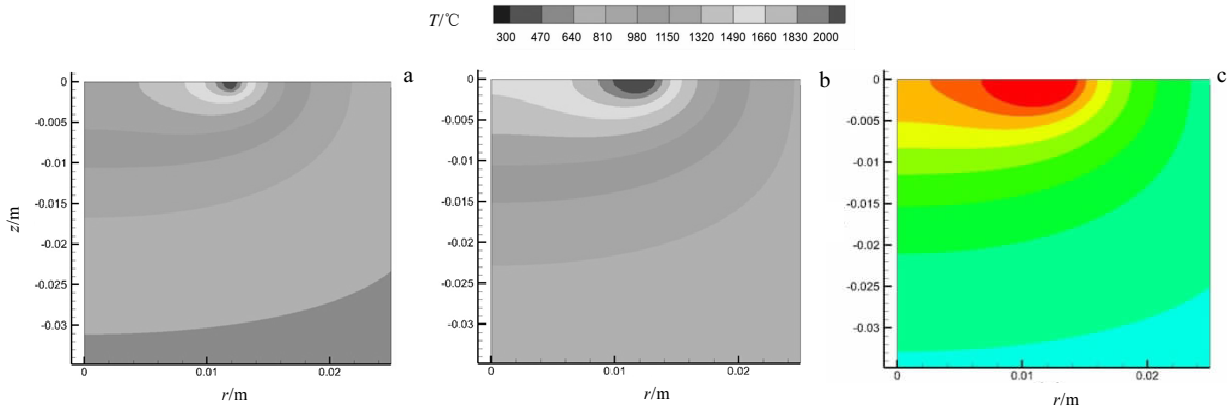

Fig.7 Temperature distribution at the scanning radius of 12.5 mm and different beam powers: (a) P_{EB}=40 kW, (b) P_{EB} =50 kW, and (c) P_{EB} =60 kW

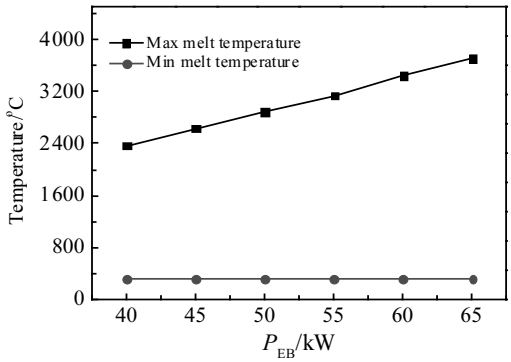

Fig.8 Maximum melt temperature and minimum melt temperature vs the beam power at the scanning radius of 12.5 mm

As discussed above, the optimum parameters of electron beam melting process of V-4Cr-4Ti alloy can be obtained according to the simulation results with a scanning radius of 12.5 mm and beam power of 60 kW. To validate the model, experiments were carried out to observe the removal of the volatile impurities using the optimum melting parameters. Fig.9 shows the as-cast microstructure of V-4Cr-4Ti alloy using different parameters. The removal of main impurities is listed in Table 2. It can be seen that the removal of the volatile impurities increases under the optimum parameters, and the simulation results are proved by the measurements.

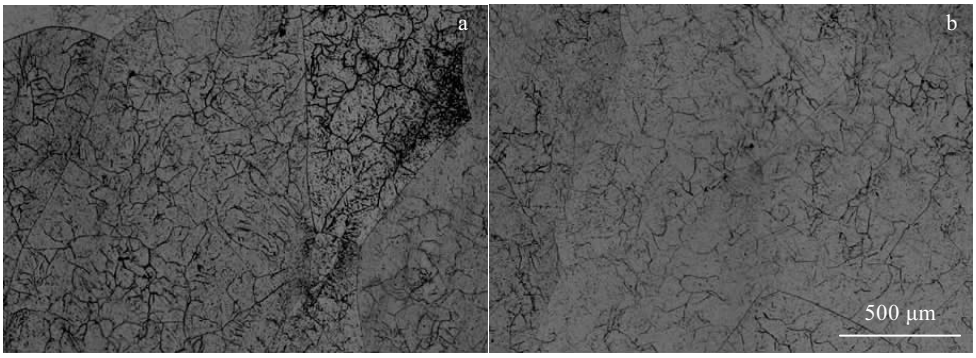

Fig.9 As-cast microstructure of V-4Cr-4Ti alloy using different melting parameters: (a) original and (b) optimum

Table 2 Removal of main impurities of V-4Cr-4Ti alloy (μg/g)

Element	ω_{raw}	$\omega_{original}$ (average)	$\omega_{optimum}$ (average)
C	100~150	60	35
N	50~80	40	20
O	450~500	420	360
Al	40~60	30	17
Fe	130~180	160	130

Note : ω_{raw}-impurity content of raw material, $\omega_{original}$-impurity content of molten ingot using original parameters, $\omega_{optimum}$-impurity content of molten ingot using optimum parameters.

3 Conclusions

1) The temperature and shape of the molten pool are influenced by the melting power and scanning radius. As the melting power increases, the maximum melt temperature increases linearly and the width and depth of molten pool gradually increase. As the scanning radius increases, the maximum melt temperature increases first and then decreases.

2) The optimum values of electron beam melting process for V-4Cr-4Ti alloy can be obtained according to the simulation results, which are scanning radius of 12.5 mm and beam power of 60 kW. The accuracy of the model is validated by the experimental data.

References

1 Muroga T. *Materials Transactions*[J], 2005, 45(3): 405

2 Muroga T, Nagasaka T, Abe K *et al*. *Journal of Nuclear Materials*[J], 2002, 307-311(2): 547

3 Potapenko M M, Drobishev V A, Filkin V Y *et al*. *Journal of Nuclear Materials*[J], 1996, 233-237(96): 438

4 Li Yufei, Luo Chao, Wang Zhigang *et al*. *Rare Metal Materials and Engineering*[J], 2008, 37(12): 2152 (in Chinese)

5 Li Yufei, Luo Chao, Wang Zhigang *et al*. *The Chinese Journal of Nonferrous Metals*[J], 2008, 18(5): 805 (in Chinese)

6 Vutova K, Koleva E, Mladenov G. *International Review of Mechanical Engineering*[J], 2011, 5(2): 257

7 Vutova K, Vassileva V, Koleva E *et al*. *Metals*[J], 2016, 6(11): 287

8 Vutova K, Mladenov G. *Vacuum*[J], 1999, 53(1-2): 87

9 Tang Ning, Sun Changbo, Zhang Hang *et al*. *Rare Metal Materials and Engineering*[J], 2013, 42(11): 2298 (in Chinese)

10 Maijer D M, Ikeda T, Cockcroft S L *et al*. *Materials Science and Engineering A*[J], 2005, 390: 188

11 Luo Lei, Mao Xiaonan, Lei Wenguang *et al*. *The Chinese Journal of Nonferrous Metals*[J], 2010, 20(S1): 404 (in Chinese)

12 Tan Yi, Wen Shutao, Shi Shuang *et al*. *Vacuum*[J], 2013, 95(9): 18

13 Liu Wensheng, Liu Shuhua, Long Luping *et al*. *Chinese Journal of Rare Metals*[J], 2014, 38(4): 666 (in Chinese)

基于有限元法的钒合金电子束熔炼过程数值模拟研究

苏　斌，陈道明，王震宏，马　荣，李鱼飞，夏胜全

(中国工程物理研究院，四川 江油 621907)

摘　要：基于 ANSYS 有限元软件建立了钒合金电子束熔炼过程的数理模型，对 V-4Cr-4Ti 合金电子束熔炼过程进行了数值模拟，研究了不同熔炼工艺参数下的熔炼过程温度场分布规律以及熔池形状。结果表明：熔炼过程温度场分布及熔池形状受到熔炼功率及扫描半径的影响。随着熔炼功率的增大，熔池最高温度将会线性增大，熔池宽度和深度将会逐渐增大。随着扫描半径的增大，熔池最高温度将会先增大后减小，通过分析获得了 V-4Cr-4Ti 合金电子束熔炼的最佳工艺参数。实验结果表明，在优化后的工艺条件下，钒合金电子束熔炼铸锭质量得到一定提升。

关键词：电子束熔炼；钒合金；温度场；数值模拟

作者简介：苏 斌，男，1985 年生，博士，高级工程师，中国工程物理研究院材料研究所，四川 江油 621907，电话：0816-3626860，E-mail: sub703@126.com